Marine Geophysical Researches **20:** 73–94, 1998.

A real-time observation network of ocean-bottom-seismometers deployed at the Sagami trough subduction zone, central Japan

Takao Eguchi, Yukio Fujinawa, Eisuke Fujita, Sin-Iti Iwasaki, Isao Watabe & Hiroyuki Fujiwara
National Research Institute for Earth Science and Disaster Prevention (NIED), 3-1, Ten-nodai, Tsukuba, Ibaraki 305-0006, Japan

Received 2 December 1997, accepted 31 August 1998

Key words: real-time observation network, ocean-bottom-seismometer, velocity seismometer, accelerometer, tsunami sensor, pressure data, tsunami record, P- and S-waves, hypocenter determination, Sagami trough, subduction zone, Tokyo metropolitan area, Philippine sea plate

Abstract

We installed a real-time operating regional observation network of Ocean-Bottom-Seismometers, connected to an electro-optical fiber communication cable, at the Sagami trough subduction zone, just south of the Tokyo metropolitan area, central Japan. The network, called ETMC, has six seismic observation sites at approximately 20 km spacing. In addition, there are three tsunami observation sites along the ETMC network to monitor the propagation process of tsunamis around the Sagami trough region.

The on-line data from the ETMC has been improving the detection capability of smaller-magnitude earthquakes even at areas close to the margin of the trough. The ETMC data analyzing system, which has a function of real-time digital filtering for each seismic channel, can read the arrival times of P- and S-waves precisely, constraining well the automatic on-line hypocenter locations. The network has been providing useful information regarding the bending and downgoing process of the Philippine sea plate at the Sagami trough subduction zone.

The pressure sensors of the installed network have a detection capability of tsunami wave trains with an amplitude of less than 1 cm. For example, the sensors recorded the full time history of tsunami wave trains, with mm order resolution, originating from a 'tsunami earthquake' with 5.7 M_W and the tsunami magnitude of 7.5 occurred near Tori Shima (Tori Is.) of the Izu-Bonin Is. arc on September 4, 1996. The maximum amplitude of the tsunami signals on the trough-floor was approximately 1 cm (P-P), in contrast with approximately 20 cm (0-P) at a coastal site on Izu-Oshima, near the trough. Also, the pressure sensors observed tsunamis due to a large tsunami earthquake (7.1 M_W) at the northern New Guinea, on July 17, 1998.

Introduction

In order to monitor seismicity in detail, associated with the plate convergence process of the Philippine sea plate at the Sagami trough subduction zone, shown in Figure 1a, we must utilize data from seismic observation sites being spatially distributed uniformly. Recently, NIED has developed an on-line regional seismic observation network with the site spacing of 20–30 km on land, in the central part of Japan, as shown in Figure 1b.

Although there was a dense seismic network on land, central Japan, in offshore areas south of Tokyo metropolitan area, including the Sagami trough, we recognized were several regional gaps in the distribution of the seismic observation sites.

The main scope of this paper is focused on the instrumentation of a new on-line operating marine seismic observation network deployed recently at the Sagami trough region. In addition, we describe briefly the data processing method as well as results of preliminary researches.

Previous studies with off-line OBSs at the Sagami trough

Seismic data obtained using pop-up type OBSs in the 1980s (e.g., Eguchi et al., 1986) revealed that marine seismic data can improve the detection rate of smaller earthquakes in and around the Sagami trough as well as the accuracy of the hypocenter locations. For example, Figures 2a and 2b represent the distribution of seismic events for the same period in 1987 (Eguchi et al., 1991). The number of events located by the off-line OBSs data is approximately nine times as large as that by data from land stations alone. Another example of the pop-up OBS survey around the Zenisu ridge, an outer-rise south of the Suruga trough subduction zone, revealed a similar result showing a larger number of OBS-located events than that exhibited by land-based network data (Eguchi et al., 1987). There have been several other pop-up OBS surveys in the Sagami trough region such as Ukawa et al. (1989). Thus, to detect and locate seismic events in offshore areas, OBS data are important in general. Furthermore, instead of the off-line observation with pop-up OBSs, an on-line seismic network is appropriate to locate the seismic events as quickly as possible.

In general, we need a uniform coverage of seismic stations both on land and in the offshore areas, in order to identify the detailed characteristics of seismicity due to the plate convergence around the Sagami trough and the Tokyo metropolitan area.

Installation of a new real-time observation network at the Sagami trough

Site survey for selecting observation sites

In general, the continental side of the Sagami trough has rough and irregular topography with faults, partly because of accretion tectonics due to the northward (or northwestward) plate convergence of the Philippine sea plate.

The initially planned route of our ‘earthquake and tsunami monitoring cable’ network, hereafter referred to as ‘ETMC,’ had a ‘zigzag’ pattern in space in order to settle the stations covering a wide area. However, for the following reasons, we modified the initial plans for the observation sites and cable route.

It was necessary to keep the cable route away from the shallow topography zones of well-known fishery areas such as the ‘Merase’ just south of Tokyo bay. Fishery activities are mostly conducted in offshore areas shallower than 800 m around Japan.

Moreover, at the axial flat zone of the Sagami trough, there are a lot of telecommunication marine cables deployed without sufficient span for ‘cable maintenance.’ The axial flat zone is only 10–20 km wide. In the case of cable maintenance such as repairing a damaged instrument or section of cable, the cable must be pulled up from the seafloor to the sea surface safely. There are plans for several new telecommunication cables to be passed through the axial zone of the Sagami trough in the next few years. Thus, we could not cross the trough axis at many points. We had to reduce the number of cable sections crossing and/or approaching other marine cables.

Taking into account the above restrictions to select observation sites of the network we carried out a site survey with acoustic profiling and piston core sampling etc. from 1992 through 1993. Using our individual site survey data, we assigned observation sites which were very close to the locations of those sites which were finally deployed, as listed in Table 1. During the survey, we investigated in detail the topography of the small areas of 3×3 km^2 surrounding the assigned sites. The maximum inclination angle of the seafloor averaged locally across the assigned observation sites was approximately less than ten degrees. Most of the sites selected are underlain not by soft or unconsolidated sediments with small S wave velocity, but by sediments consisting of sand, small-sized pebbles or small-sized rocks.

The selected route of the network approximately covers the offshore section of the interplate rupture zone of the 1923 Kanto earthquake (7.9 Ms), which severely damaged the Tokyo metropolitan area. The estimated rupture area of the 1923 event is either 95×54 km^2 (Matsu’ura et al., 1980) or 130×70 km^2 (Kanamori, 1971). This implies that the ETMC approximately delineates the shallowest portion of the rupture area. The 1923 event caused the loss of more than 140 000 people’s lives. Tsunamis accompanying this great earthquake reached 12 m in height at a coastal area west of Hiratsuka. Previously, there was no regional on-line marine seismic network at the rupture zone. The network ends at a point on the northern most part of the Philippine sea plate. Thus the ETMC starts at the continental side plate and crosses the plate boundary, reaching the oceanic plate.

Our main interest in using the ETMC data is shallow seismicity and the related dynamics at the Sagami trough subduction zone and the Izu-Bonin Is. arc and

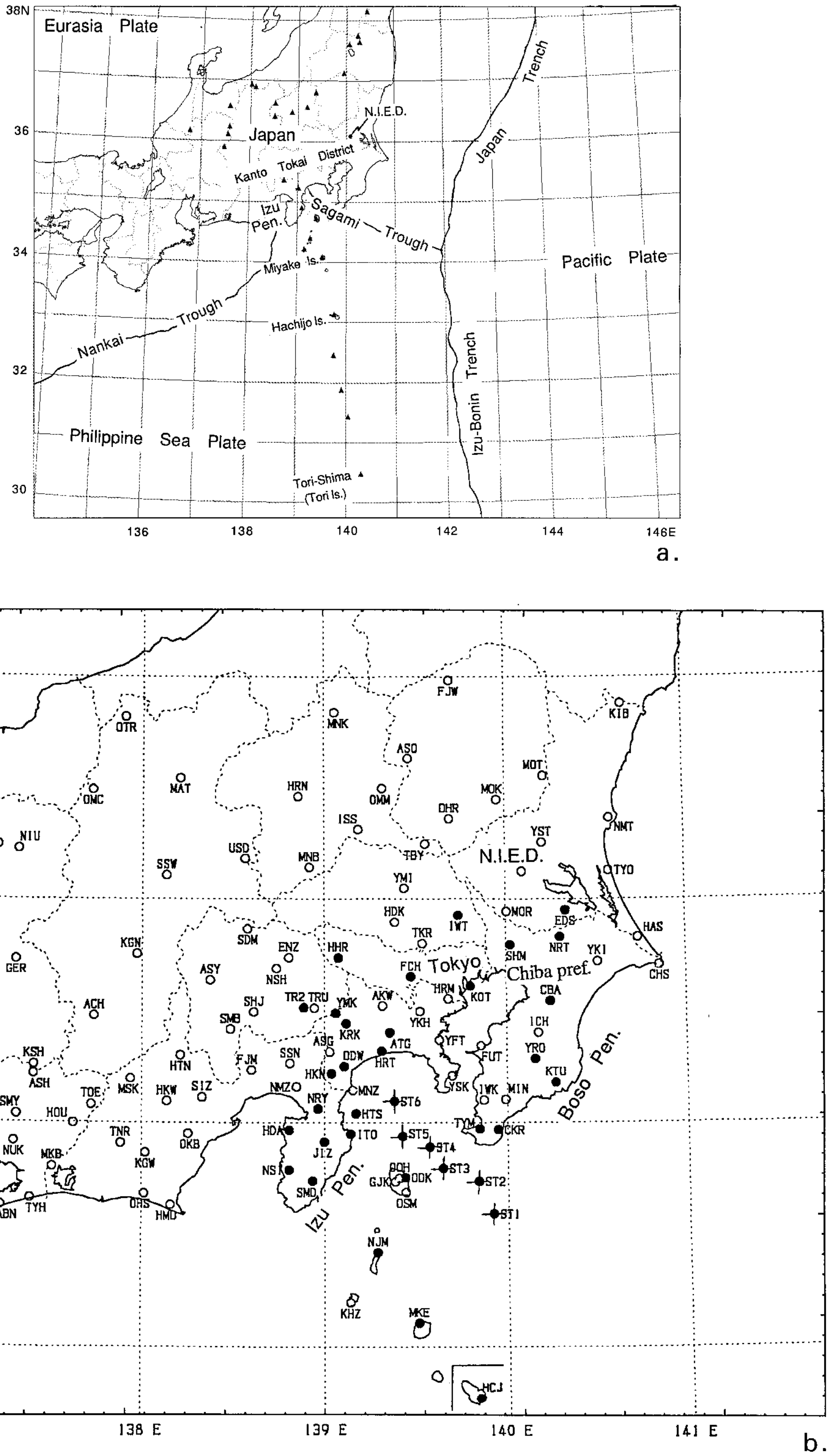

Figure 1. (a) Geometrical setting map of the Sagami trough subduction zone, central Japan. Filled triangles indicate quaternary active volcanoes. (b) The distribution of seismic observation sites (open and filled circles) on land in the Kanto and Tokai districts, central Japan. All of the sites plotted were selected by NIED to monitor the activity of microearthquakes etc. In total, there are approximately one hundred stations in the district. (*N.B.*) This map does not include the seismic stations of other organizations and institutions, such as those of JMA (Japan Meteorological Agency), universities, and local governments. (Crosses with filled circles, shown by ST1 to ST6, indicate the deployed sites of on-line operating ocean-bottom-seismometers, and the filled circles, 30 in total, are selected land stations in order to study seismicity, as shown in the later section.)

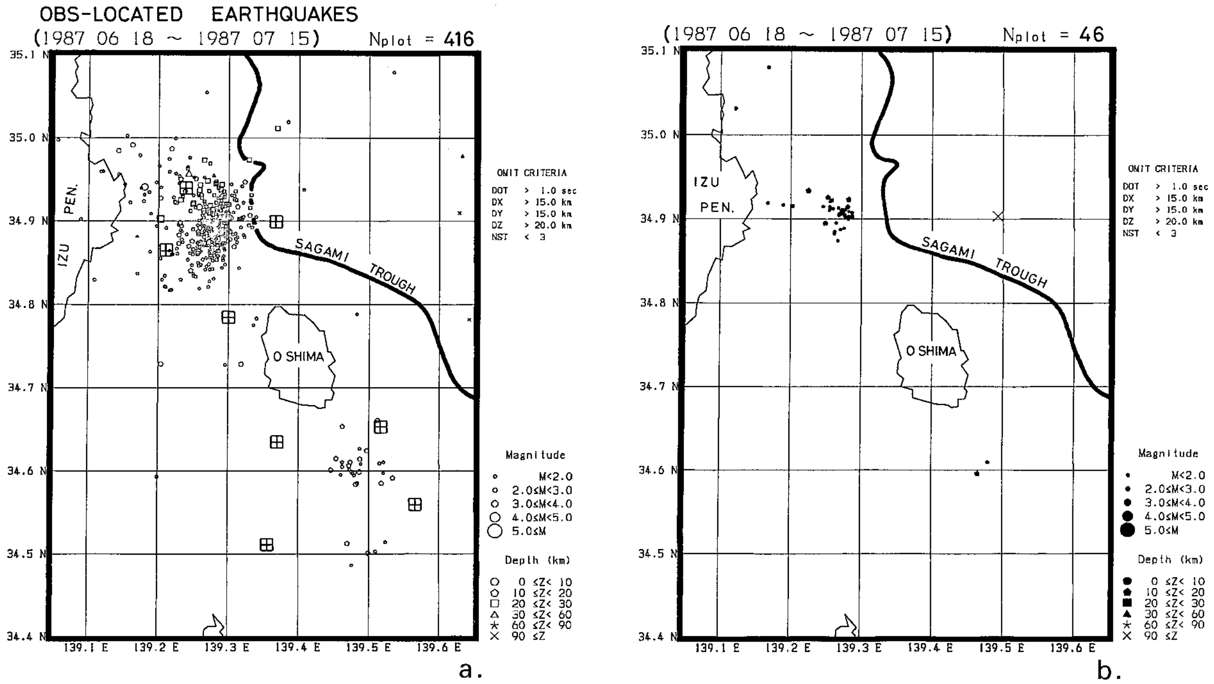

Figure 2. (a) The distribution of seismic events located with the off-line OBSs in the western part of the Sagami trough for a period from June 18 through July 15 in 1987. The total number of the events plotted is 416. Symbols of squares with crosses indicate the sites of the deployed off-line OBSs. (b) Seismic events (46 in total) by the land seismic stations for the same period.

Table 1. Location list of the observation sites along the ETMC

Sites	Longitude (deg.)	Latitude (deg.)	Depth (m)	Observation Instrument
ST1	139.922 E	34.592 N	2125	Seismometers
ST2	139.843	34.736	2165	Seismometers
ST3	139.647	34.795	875	Seismometers
ST4	139.574	34.890	895	Seismometers
ST5	139.425	34.938	1427	Seismometers
ST6	139.381	35.084	1122	Seismometers
VCM1	139.923	34.592	2138*	Pressure Sensor
			2125	for Tsunamis
VCM2	139.607	34.808	1764*	Pressure Sensor
			1780	for Tsunamis
VCM3	139.394	35.068	1232*	Pressure Sensor
			1225	for Tsunamis

The coordinate used is the 'Tokyo Datum,' which is based on the 'Bessel ellipsoid' with the equatorial radius (a) of 6 377 397.155 m and flattening (f) of 1/299.152813. The depths for ST1 through ST6 are determined using bathymetry data derived during the site survey. The bathymetry data accuracy is approximately $0.5 + 0.001\times$ depth (in m). For VCM1, VCM2, and VCM3, the depth listed with an asterisk (*) is based on its own value of the averaged water pressure on the seafloor. The accuracy of the pressure-based depth data is approximately $0.7 + 0.0001\times$ depth (in m).

trench system, as well as in the deep structure of the earth.

Manufacturing the ETMC system

By the end of February 1996, we had finished manufacturing the system of the regional observation network of Ocean-Bottom-Seismometers. In parallel, we constructed pieces of the submarine electro-optical fiber cable. The electro-optical cable adopted has twelve (low energy-loss) fibers with the transmitting optical wavelength of 1.55 micrometers, which is the same as that currently used for submarine telecommunication cables. The pieces of cable for areas with irregular topography are covered with single armor to increase the cable strength. Cable sections to be buried beneath the seafloor are protected with a single armor of tension members. A piece of cable for the coastal landing section is double armored.

Detailed descriptions of the instruments in place at observation sites along the assembled cable network are given in the later section. The total length of the network is approximately 125 km.

Cable deployment

In March 1996, we installed successfully the regional observation network at the Sagami trough subduction zone. The route of the regional network is shown in Figure 3.

During the cable deployment we adopted a software for ship navigation control, coded by Makai Ocean Engineering, Inc., in order to deploy the cable on the seafloor without deviating substantially from the planned route. The navigation control software package incorporated the data of the location of cable just set out to the seafloor, the ship's position, water current, topography, etc. The ship's position was determined with differential GPS navigation. In order to deploy the cable network along the planned route with high precision, the ship traveled at less than 2.5 nautical miles per hour. Table 1 compiles the deployed observation sites along the ETMC. Figures 4a through 4h represent the local situation of each observation site on both the planned and deployed routes of the ETMC. The detailed topography maps of the small 3×3 km^2 areas shown in Figures 4a–h are based upon our own detailed site survey data. As a result, the location of the observation sites is offset by only 106 m on average with the standard deviation of 66 m. At the leading point (close to VCM1) of the electro-optical cable, we installed an 'ocean ground electrode' ('sea earth') to form a electric current circuit throughout the insulated cable and earth.

For the route section with a depth of less than 800 m, between the Hiratsuka landing site and the ST6, we buried the cable at least 70 cm below the seafloor with the aid of a ROV (Remotery Operated Vehicle) and high pressure water jetting equipment etc. to trench the surface section of the (soft) sedimentary layer along the cable line, excepting points covered with hard rocks. This is partly to ensure the cable from fishery instruments on the seafloor. The total length of buried cable is approximately 12 km. Moreover, at the landing point along the sandy beach, we buried the section of double armored cable at a depth below the surface which would ensure that the cable remained buried even in the case of stormy weather caused by large typhoon(s). Stormy waves can scrape off the soft sand layer on the beach to a considerable extent.

The cable landing point is just south of our branch office ('Hiratsuka Test Site'). We built a station at the Hiratsuka test site to settle various electronic units such as those for data communication, DC power supply, controlling and monitoring the observation instruments etc. The new station is called 'Hiratsuka data communication station.' In the event of a problem with the communication line between Hiratsuka and Tsukuba, the Hiratsuka data communication station operates by keeping an auxiliary data backup recording system.

The deployment of the ETMC, on both the overriding and downgoing plates, in the Sagami trough subduction zone removed the regional gap in the distribution of seismic observation sites.

Observation sites on the ETMC

Seismic observation sites

The ETMC has six seismic observation sites at approximately 20 km spacing. Figure 5a shows the block diagram of the seismic observation instruments. The cylindrical pressure vessel used is approximately 1.6 m long, with a diameter of 26 cm (Figure 5b). To record seismic signals in a wide dynamic range, each observation site has two types of sensors, namely, a short period velocity seismometer (covering the frequency range of 1–30 Hz (-3 dB), and amplitude up to 83 milli-kine) and an accelerometer (covering 0.05 to 30 Hz (-3 dB), and up to 500 gal). Here, 1 kine is 1 cm s^{-1}, which is a frequently used unit in seismology, and 1 gal is 1 cm s^{-2}. Both sensors have a dynamic range of 18 bits or more, and are produced by the Akashi Co., Kanagawa, Japan. Each of the sensors is mounted on a gimbal to adjust the vertical sensor axis. The acceleration sensor operates with a electric feed-back process. The analogue electric signals from the sensors are multiplexed into digital data and then transformed into optical signals.

The two types of seismometers also function mutually as backup sensors in the event of any problem with either of the instruments at the observation site.

To obtain high quality earthquake data, we attached a 'seismic coupling cover' on the pressure vessel (Figure 5c). The coupling cover might constrain the freedom in the rotational motion of the cylindrical vessel to some extent, because the vessel without the cover contacts itself with the seafloor in a limited linear area. We expect that the non-cylindrical shaped cover will improve the seismic coupling between the seafloor and the sensors, especially in the direction normal to the vessel's axis.

Moreover, we put additional cylindrical weights on the cable surface of both sides of the pressure vessel,

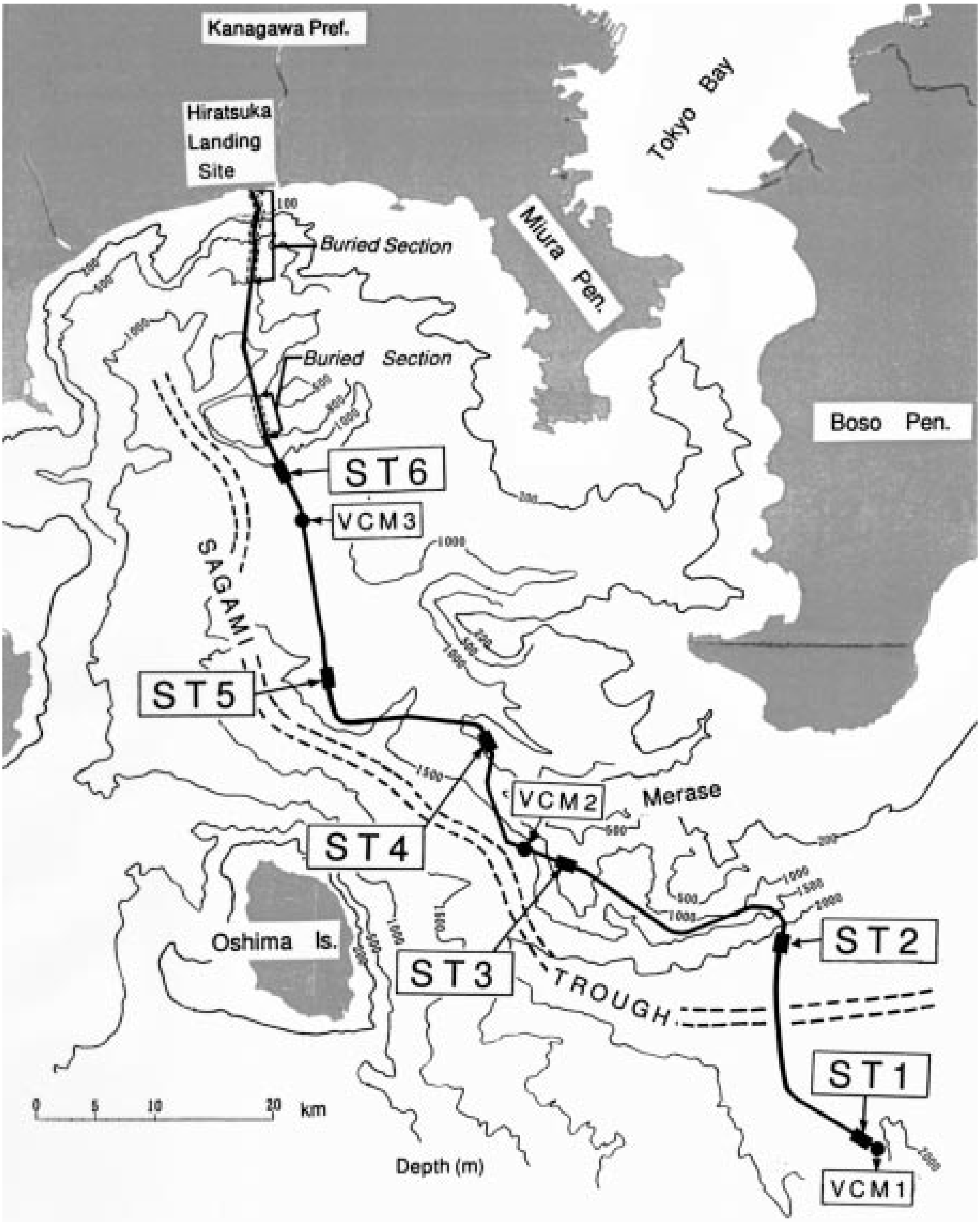

Figure 3. The route map of the ETMC. Curved, parallel, and dashed lines represent the axial zone of the Sagami trough. The ETMC comes ashore at Hiratsuka.

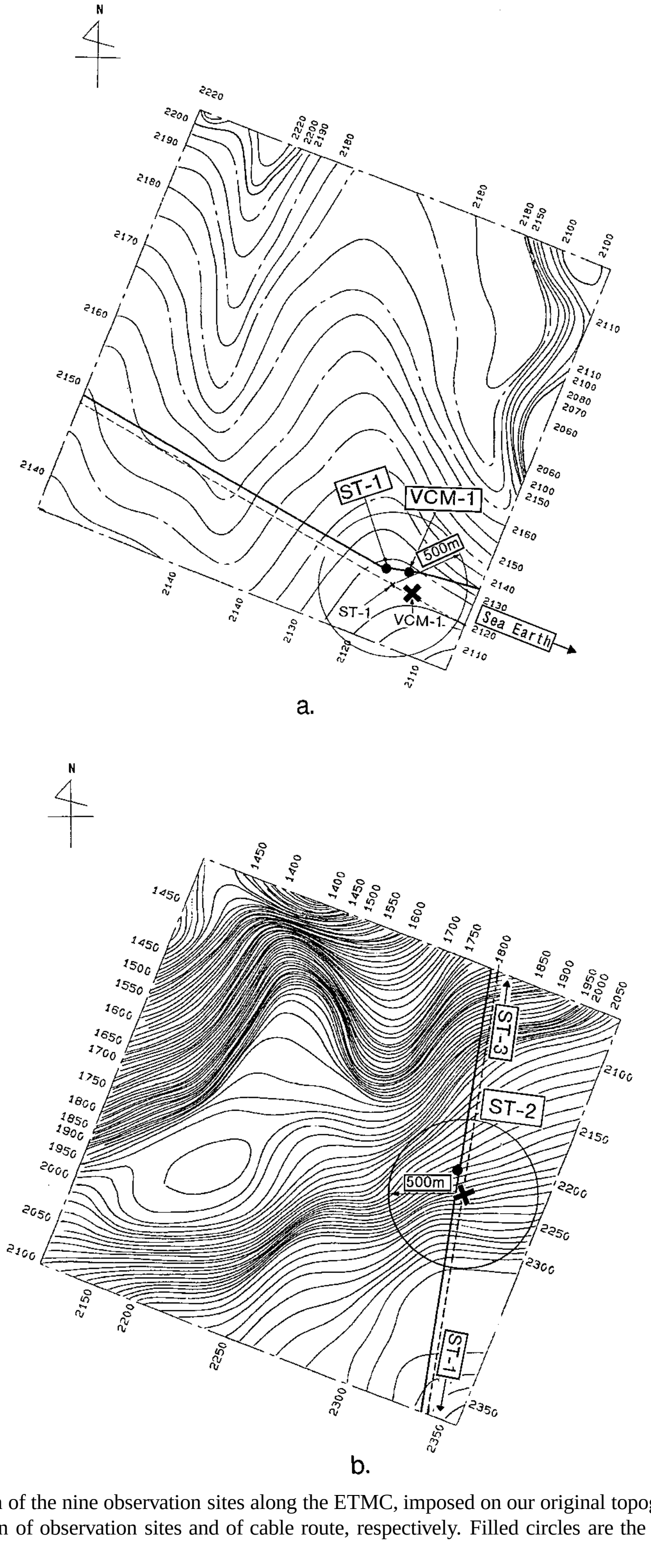

Figure 4a–h. The locality of each of the nine observation sites along the ETMC, imposed on our original topography map. Crosses and dashed lines indicate the planned location of observation sites and of cable route, respectively. Filled circles are the actual sites installed, solid lines show the actual deployed cable route. Contour lines of topography are in meters. It must be noted that the observation sites to be deployed were carefully assigned using our individual relief map of the subduction zone with irregular surfaces.

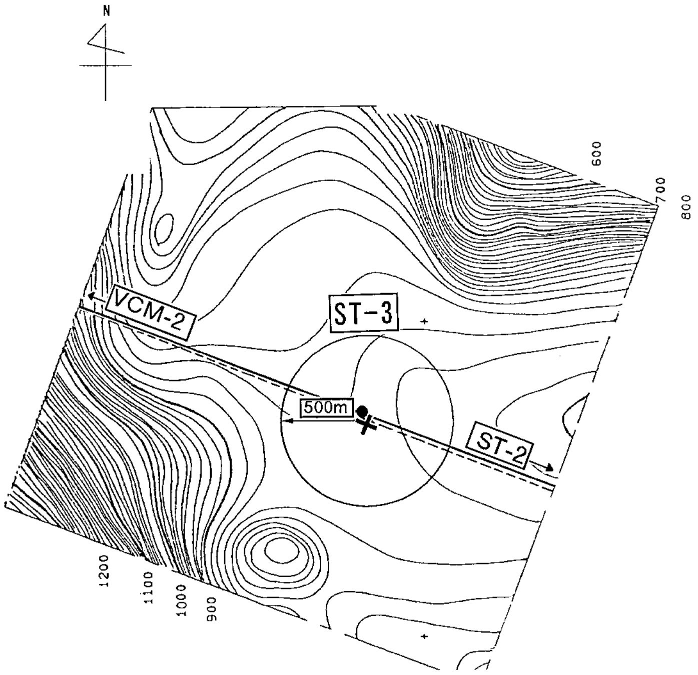

c.

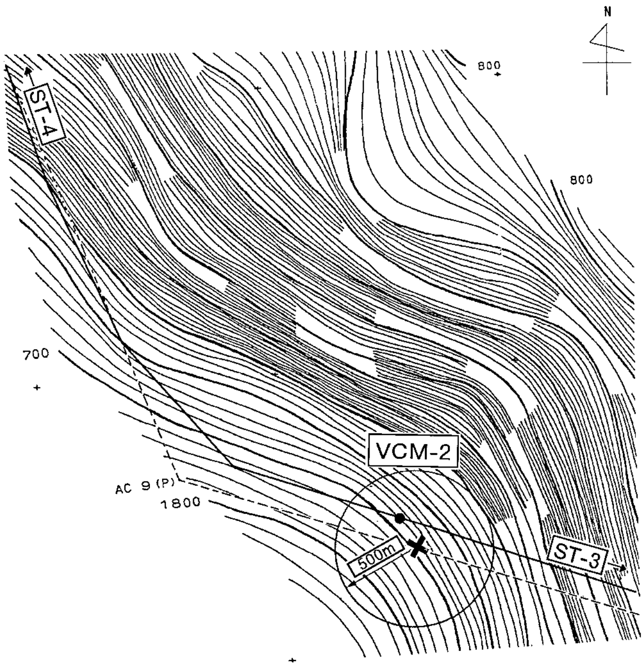

d.

Figure 4. Continued.

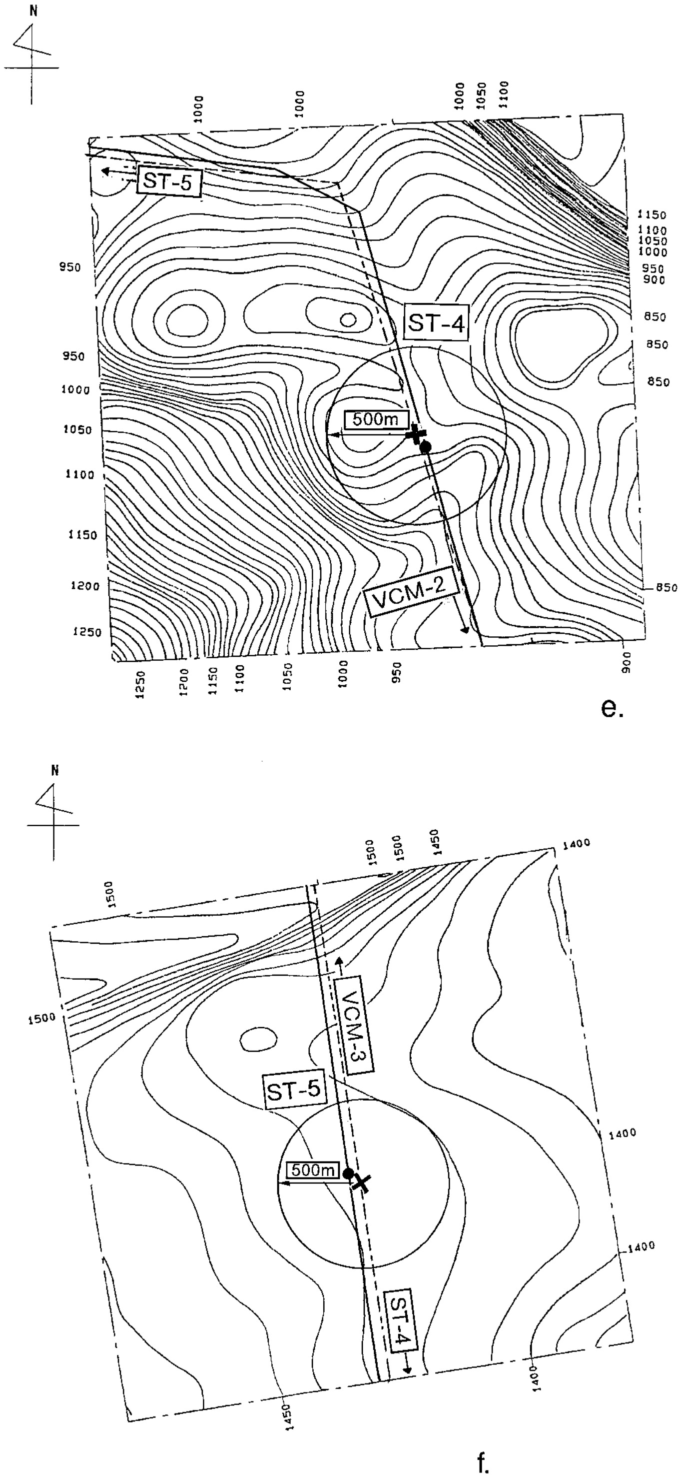

Figure 4. Continued.

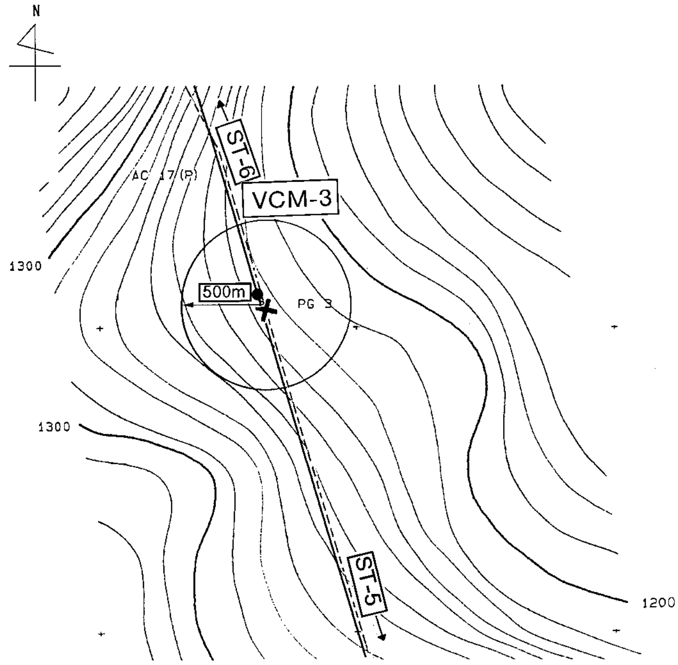

g.

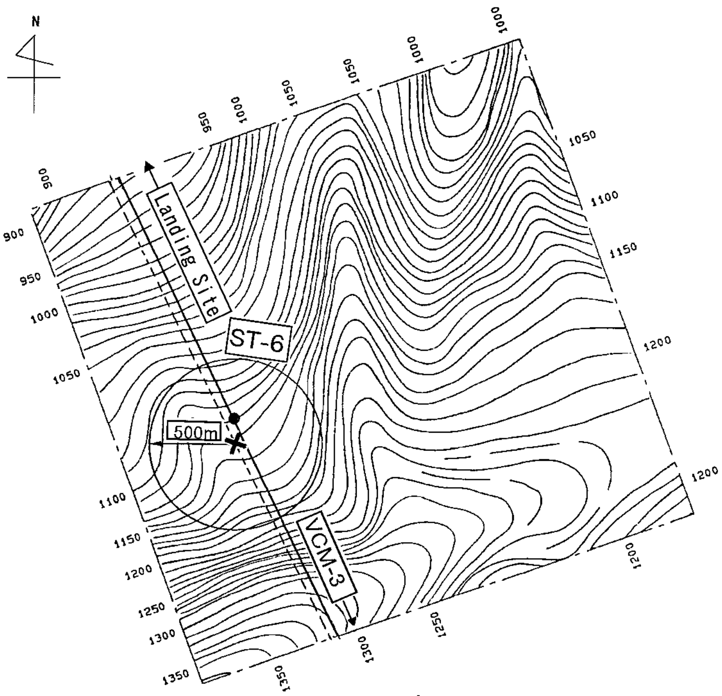

h.

Figure 4. Continued.

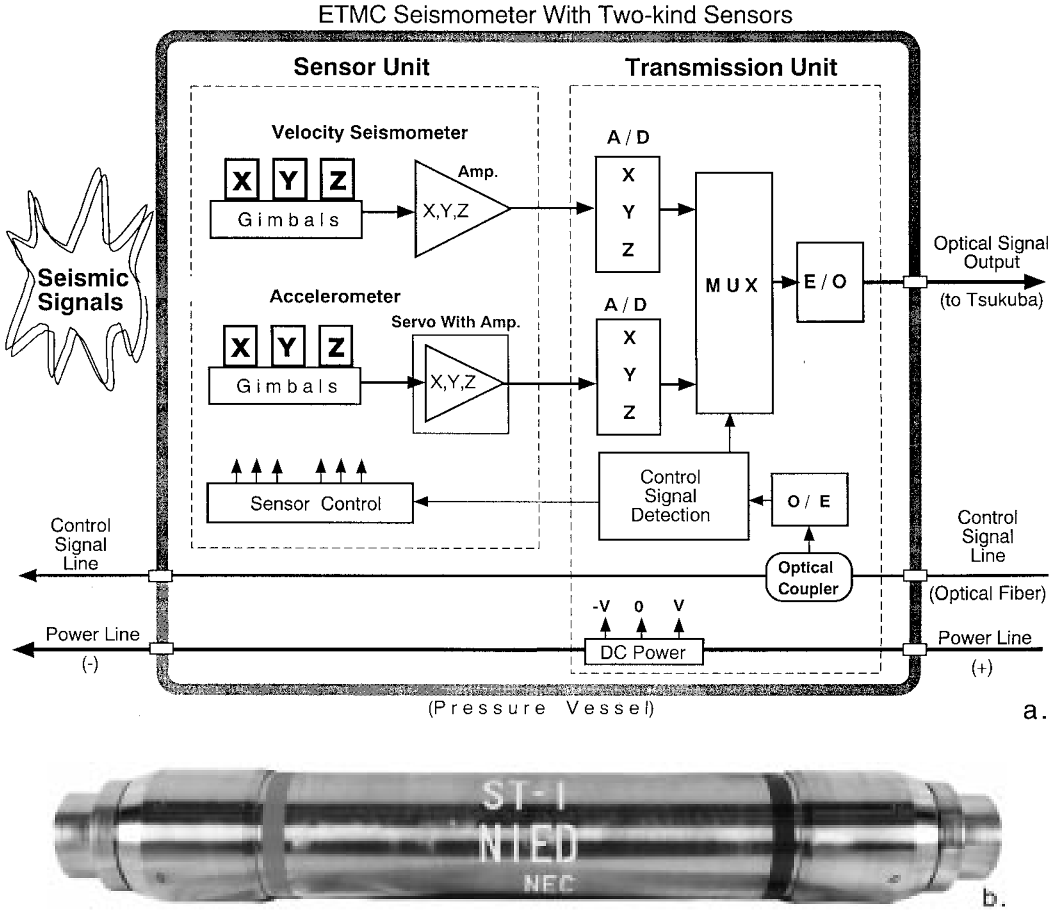

Figure 5. (a) Block diagram of the seismic observation instruments. (b) External view of the seismic observation instruments with the two types of sensors. The weight is 310 kg in air (235 kg in water). (c) Seismic coupling cover. The weight is 250 kg in air (225 kg in water), and the total width is approximately 1 m. (d) The total configuration and dimension of the seismic observation instruments settled on the sea-floor.

to improve the seismic coupling and S/N. The cylindrical weight used is made of rubber ballasts. Each of the cylindrical weights is approximately 7 m long and weighs 48 kg (in water), that is, the sensor vessel with the coupling cover is connected to the weighted cables not to the normal submarine cables. Without the cylindrical weight, the motion freedom of the cable alongside the vessel cannot be fully constrained especially during large earthquake motions, because of a small amount of negative buoyancy of the armor-less cable alongside the vessel on the sea bottom. Figure 5d shows the detailed dimension of the seismic observation instruments with the coupling cover and the nearby cable with the additional cylindrical weights.

After finishing the deployment of the ETMC onto the seafloor, we sent a gimbal control command to shift all the seismic sensors from the lock mode to the free mode. Then, the ETMC adjusted itself to the horizontal level of the seismic sensors within the pressure vessel to attain an appropriate geometrical configuration for seismic recording. The averaged noise level (0-P) is mostly smaller than several micro-kine on the vertical component velocity seismometer, contributing to improve the degree of detection rate of microearthquake activity associated with the convergence process of the Philippine sea plate against the continental plate around the Sagami trough region.

Tsunami observation sites

At three separate points along the ETMC, we installed a water pressure sensor and thermometer to monitor the propagation process of tsunamis around the Sagami trough region (Figure 3).

The block diagram of the tsunami observation instrument is plotted in Figure 6a. The pressure sensor

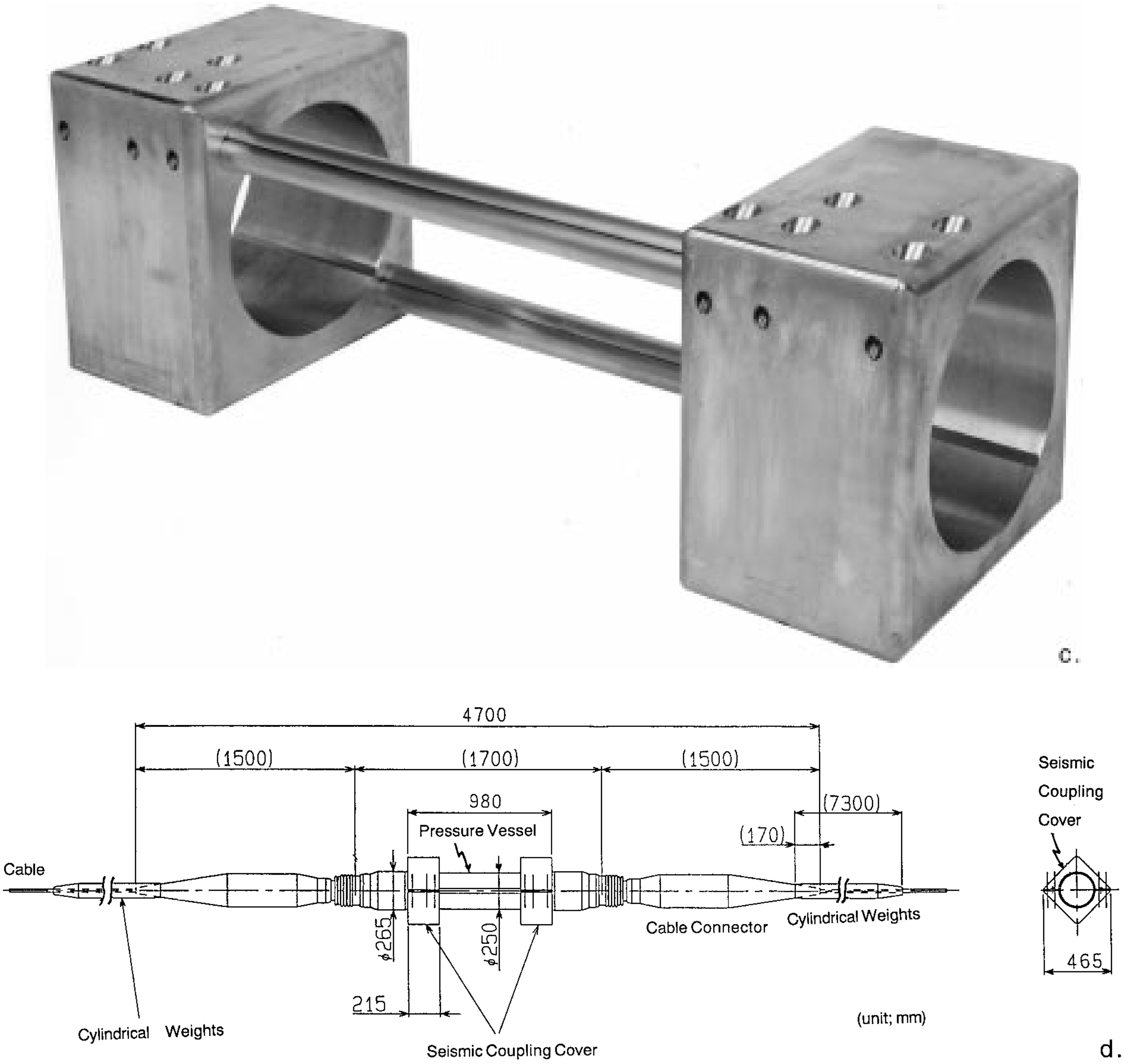

Figure 5. Continued.

consists of two quartz oscillators. The pressure oscillators adopted are HP 2813E. One oscillator is for measuring pressure change, the other for calibrating the temperature dependence of the quartz oscillator. To calibrate the temperature change precisely, every effort was made to locate the two quartzes at a similar thermal situation within the vessel. The outermost vessel, in which the pressure sensor etc. is mounted, is 2.2 m long, with a diameter of 26 cm (Figure 6b). Moreover, the oscillator was covered with a cylindrical oil tank, which raised the thermal capacity, in order to reduce and diffuse the influence of unsteady temperature changes on the surface of the outermost vessel. Occasionally, the data from the tsunami sites show temperature changes (P-P) of 0.1 to 0.4 °C. To get tsunami signals with mm order resolution, the raw data of quartz oscillations has to be carefully transformed using calibration constants for each oscillator. A calibrated tsunami data example with mm order resolution will be given in a later section.

Our tsunami observation system is a revised version of a model which was assembled by the MRI (Meteorological Research Institute, Japan) in the 1970s (MRI, Japan, 1980). The tsunami observation instrument by MRI was mounted with so-called 'co-axial cable'. Currently, there is no plan to lay a new network with co-axial cable in Japan. Our optical fiber cable, therefore, inevitably forced the revision of the old MRI type tsunami observation system. We modified the tsunami observation instrument to identify tsunami signals with an amplitude resolution of 1 mm order so that the pressure sensor can provide useful data for changes in sea level for a time scale less than years as well as the vertical components of crustal deformation. To study the long term pressure change in a scale of years, however, we must incorporate other kinds of information of secular changes in the individual oscillation constants of the quartzes within the vessel. However, at present, we have no data on the secular change characteristics of the oscillation constants. Nonetheless, changes in the sea level and vertical crustal deformation at a temporal range less than years can now be observed.

Data transmission and format

There are a total of 12 optical fibers along the ETMC. The data observed at each of the observation sites on the seafloor are transmitted through an individually assigned optical fiber cable among the 12 fibers. The seismic and tsunami observations sites thus utilize nine fibers in total. One of the other three fibers is used for transmitting system control and monitoring signals. In the event of fatal damage anywhere along the 125 km long cable, signals are transmitted into the remaining two fibers to identify the location of the damaged part(s) by measuring the back-scattering signals. The digital sampling frequency of the data is 8 KHz and the total dynamic range of each channel is 16 bits, between the seafloor observation sites and the Hiratsuka data communication station.

Data transmission from Hirastuka to NIED, Tsukuba

At the Hiratsuka data communication station, the data from the submarine cable are transformed into another format to transmit to the 'Tsukuba data station' through a land-based digital commercial telecommunication line. The on-line commercial telecommunication line adopted has a transmission capacity of 192 kbs (kilo-bits per second). During the data transformation at the Hiratsuka station, the dynamic range of the seismic signals is improved from 16 to 20 bits using a kind of low pass digital filtering process from 8 KHz data to 200 Hz (100 Hz) for the velocity data (for the acceleration data). However, due to noise during low pass digital filtering, we think that the reliable dynamic range is not 20 bits but the upper 18 bits. In the case of a reliable dynamic range of the upper 18 bits, the LSB (least signal bit) corresponds to 0.6 micro-kine and 1.9 mgal for the velocity seismometer and accelerometer, respectively. In addition, the pressure and temperature data from the tsunami observation sites are superimposed within the 192 kbs line. The sampling frequency of the tsunami related data is 10 Hz.

The data transmitted from the seafloor to the Tsukuba data station are never transformed into analogue format, maintaining the original forms recorded by the sensors on the seafloor.

Data analysis and preliminary results

Hereafter, we explain the analysis at the 'Tsukuba data station', and present the preliminary results of local seismicity and tsunamis based on the ETMC network. The original data of horizontal components from the two types of seismometers are not aligned to the N–S and E–W, because one of the horizontal seismometers is oriented to the axial direction of the pressure vessel. The axial direction of the vessels is not uniform, as is obvious from Figure 3. The original horizontal seismic data are transformed into N–S, E–W components. To remove noises on each channel of the seismic records, on-line digital filtering is applied before the automatic hypocenter locating stage.

Currently, a band-pass filter of 5 to 15 Hz is set for the velocity seismometer data. For accelerometer data, a low pass filter (fc = 15 Hz) is applied. The above filter range was determined after analyzing the spectra of noises superimposed on the data from each seismic channel data.

Figure 7 lists current research themes based on the ETMC data, etc., as well as the data transmission flow.

The data from the velocity seismometer is used for the local seismicity study including the inversion of the 3-D seismic velocity structure around the Sagami trough. The accelerometers, which provide relatively long term information, might contribute to the source process study of moderate sized earthquakes and possibly to strong motion seismology.

Hypocenter determination with the ETMC data

Figures 8a and 8b show the wave trains of a recent earthquake (6.6 M_{JMA}) which occurred at east off

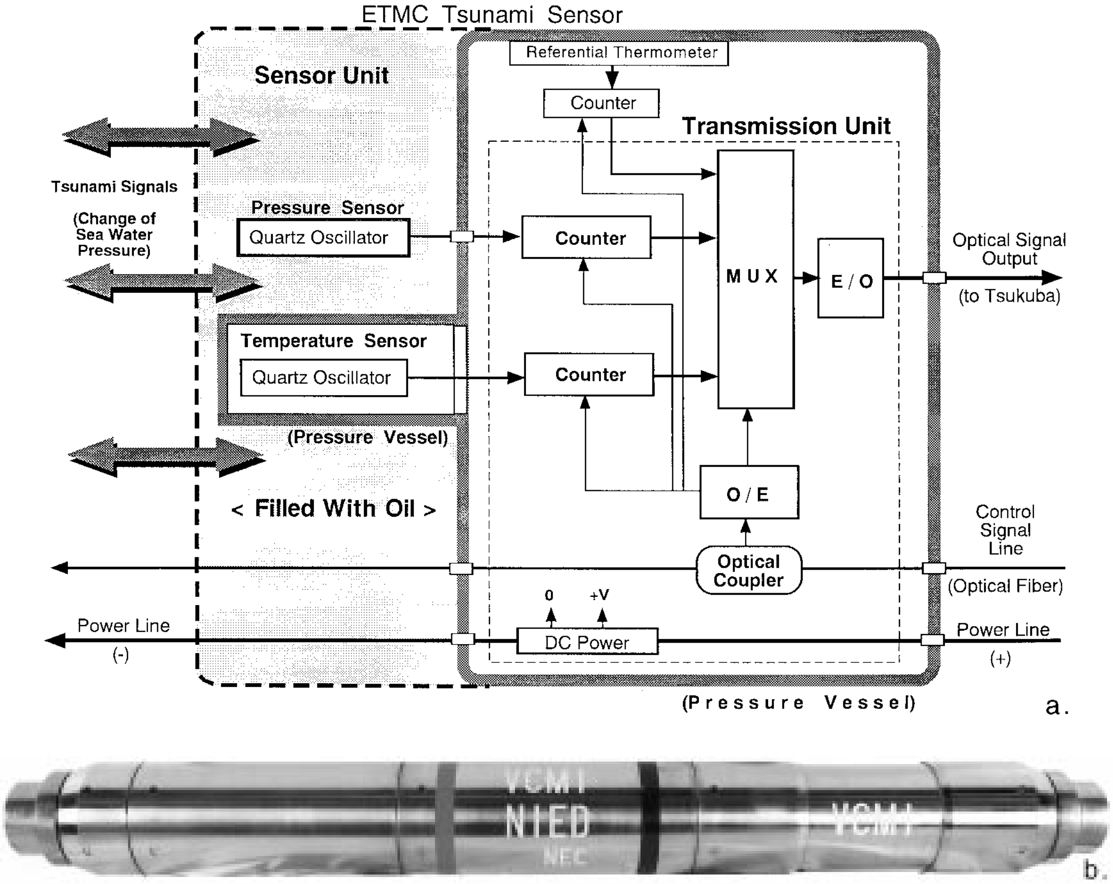

Figure 6. (a) Block diagram of the tsunami observation instrument. (b) Outermost view of the tsunami observation instrument. The total weight is 410 kg (290 kg) in air (water).

Chiba prefecture on September 11, 1996. The event occurred within the downgoing Pacific plate from the Japan trench subduction zone. The data observed suggest that the maximum horizontal acceleration during the event was approximately 30 gal at the Sagami trough. But there is some uncertainty regarding the above value of the maximum acceleration due to the limited seismic coupling between the pressure vessel and the seafloor.

The ETMC data are continuously transmitted from the seafloor, through the Hiratsuka coastal data transmitting station to the data center at NIED in Tsukuba. We developed a software package to process and analyze the seismic and tsunami data at the Tsukuba data station. There are operating software packages for both on-line and off-line modes. Hereafter the operating softwares will be referred to as the system. We utilize the data from the ETMC as well as from land stations surrounding the Sagami trough subduction zone, in order to improve the resolution of hypocenter determination. Currently our system can process the data from a maximum of thirty-six points, that is, the six ETMC sites and thirty land stations (see Figure 1b).

As is generally recognized in the research field of local seismicity, the seismic ground noise level is high on ocean islands as well as on land areas close to the coast, mainly because of seismic tremors with characteristics similar to seismic surface waves. For example, the long-term averaged seismic noise level (rms) of the U/D component of velocity seismometers at the coastal land sites and oceanic island stations, shown in Figure 1a, are larger than 10 and 20 micro-kine, respectively. However, all of the six seismic stations of the ETMC indicate that the long-term averaged seismic noise level (rms) of the U/D component is less than 10 micro-kine. When the influence of noise due to various ships, which are passing through the route

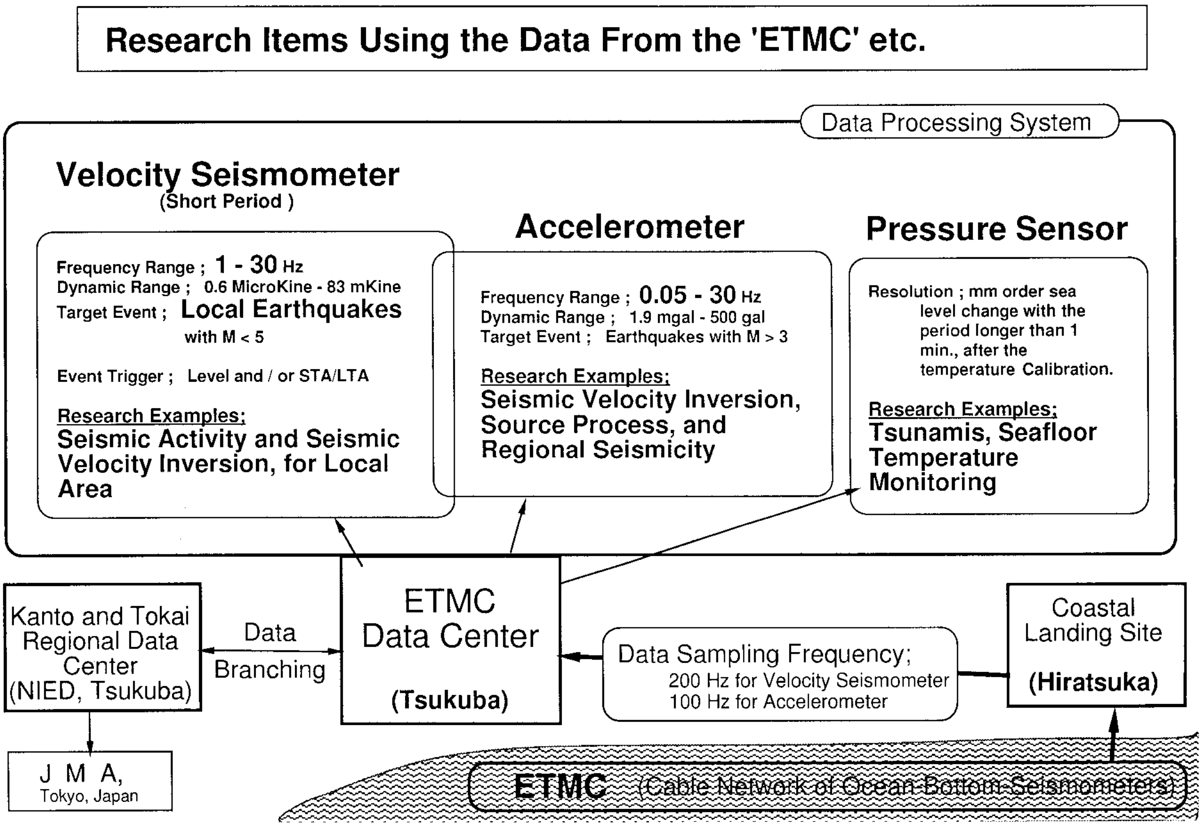

Figure 7. Research items using ETMC data, etc., and the data transmission flow from the seafloor to NIED in Tsukuba.

crossing the Sagami trough, is removed, the noise level (rms) of the U/D component becomes less than 5 micro-kine. To get accurate information regarding microeathquake wave forms, it is necessary to develop seismic stations with a U/D noise level less than several micro-kine.

The hypocenter locating process for local or regional seismic events is one of the important research items based on ETMC data. Our main target events are those which occur at the Sagami trough subduction zone and the vicinity to the south which includes the northern part of the Izu Bonin trench subduction zone. In other words, we are interested in earthquakes with the approximate epicentral distance from the ETMC is less than 100 km to the north and west, 300 km to the east, and 400 km to the south, with the hypocenter depth shallower than 300 km. Thus, the seismic wave trains for our local events at the Sagami trough have a time interval between P- and S- waves, that is an S-P time of less than 40 s. Regional target events may have an S-P time less than 60 s. Hereafter we briefly explain the event locating processes such as the automatic identification method of P- and S-wave arrival times for these events.

At first, the system automatically locates the hypocenter of seismic events within wave train data which are commonly triggered at more than two stations. After the digital filtering process of seismic record sections, the system automatically reads the arrival times of P- and S-waves as well as the maximum amplitude for the data at each station. The system estimates the P-wave arrival later than the time of ‘trigger on’ for each seismic event, by using algorithms including criterion condition for the ratio of LTA and STA and an AR (auto regressive) logic. Here, LTA and STA are long term and short term averaged values of amplitude data, respectively. During the statistical process to estimate the P- and S-wave arrivals, the system uses the squared values as time series data, not the original amplitude data.

To automatically find S-wave arrivals from local earthquakes with an S-P time smaller than 40 s, we adopted a new method as follows: The S-time is later than the P-time and before the arrival of the maxi-

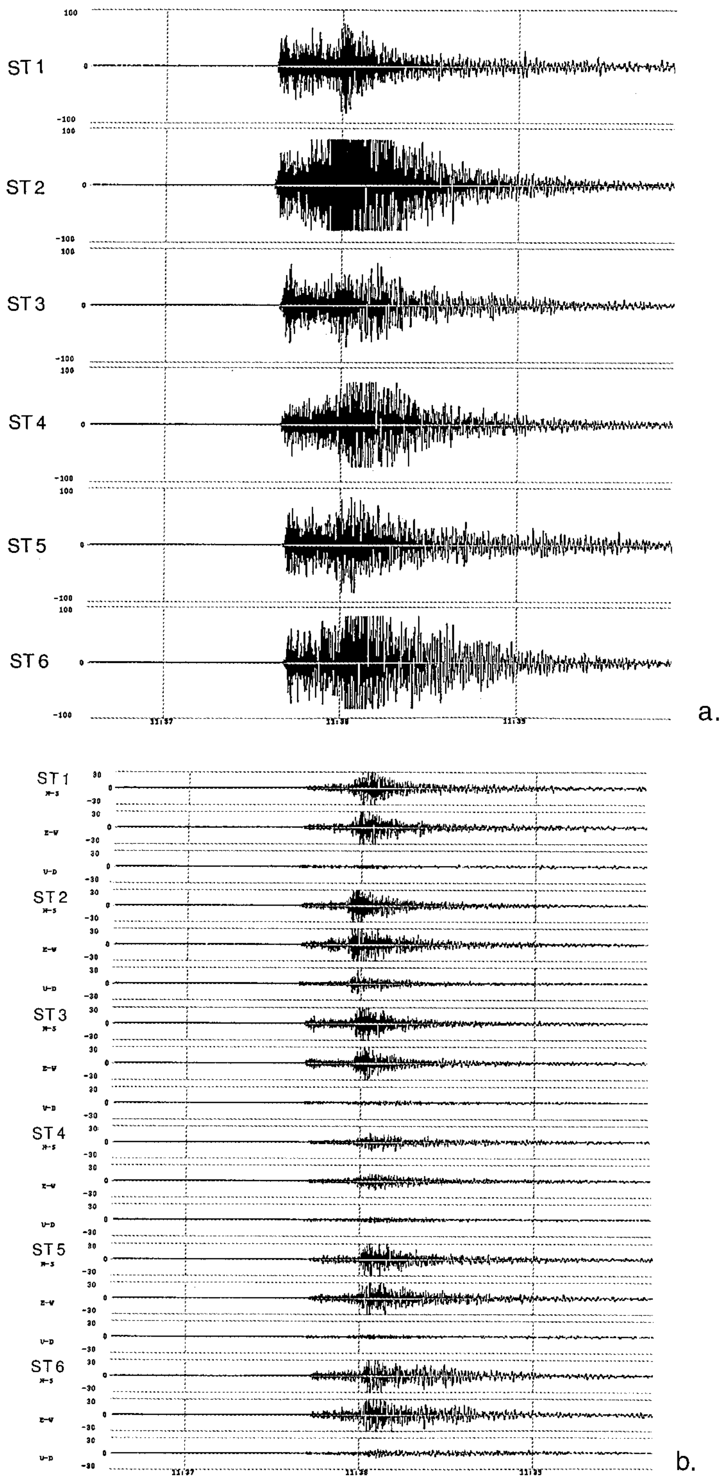

Figure 8. (a) Recent seismic data of an earthquake (6.6 M_{JMA}) at east off Chiba prefecture on September 11, 1996. Up-down component data from the velocity seismometers are plotted with the 0-P scale of 100 micro-kine. (1 kine = 1 cm s^{-1}.) It should be noted that the maximum amplitude of the velocity seismometer is 83 milli-kine. The top line is ST1 through ST6 at the bottom. The total horizontal range is 5 min. (b) Accelerometer data for the recent earthquake shown in Figure 10. Three component data (N–S, E–W, U–D) on the accelerometer are plotted with the 0–P scale of 30 gal. The top three lines are of ST1 through ST6 at the bottom.

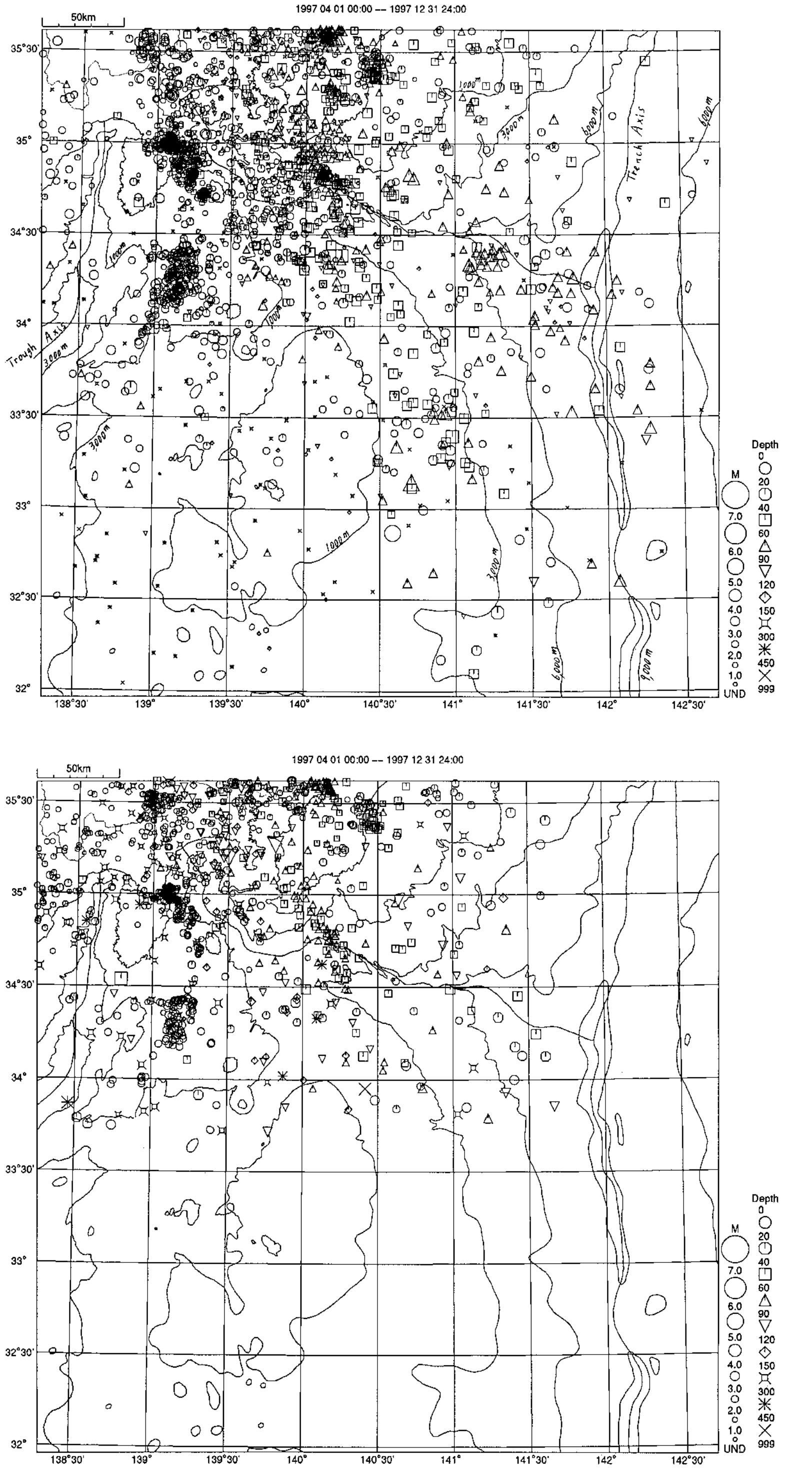

Figure 9. Results of the automatic hypocenter calculation for events during nine months from April 1 through December 31, 1997. (There were several intermittent periods of data intermission.) (a) Events (2274 in total) based on the seismic data of both the six ETMC sites and the nearby thirty selected land stations of NIED. The sites used are shown in Figure 1b. (b) Hypocenters (1267 in total) obtained mainly from the data of NIED land stations in the Kanto-Tokai region. The land stations are shown in Figure 1b.

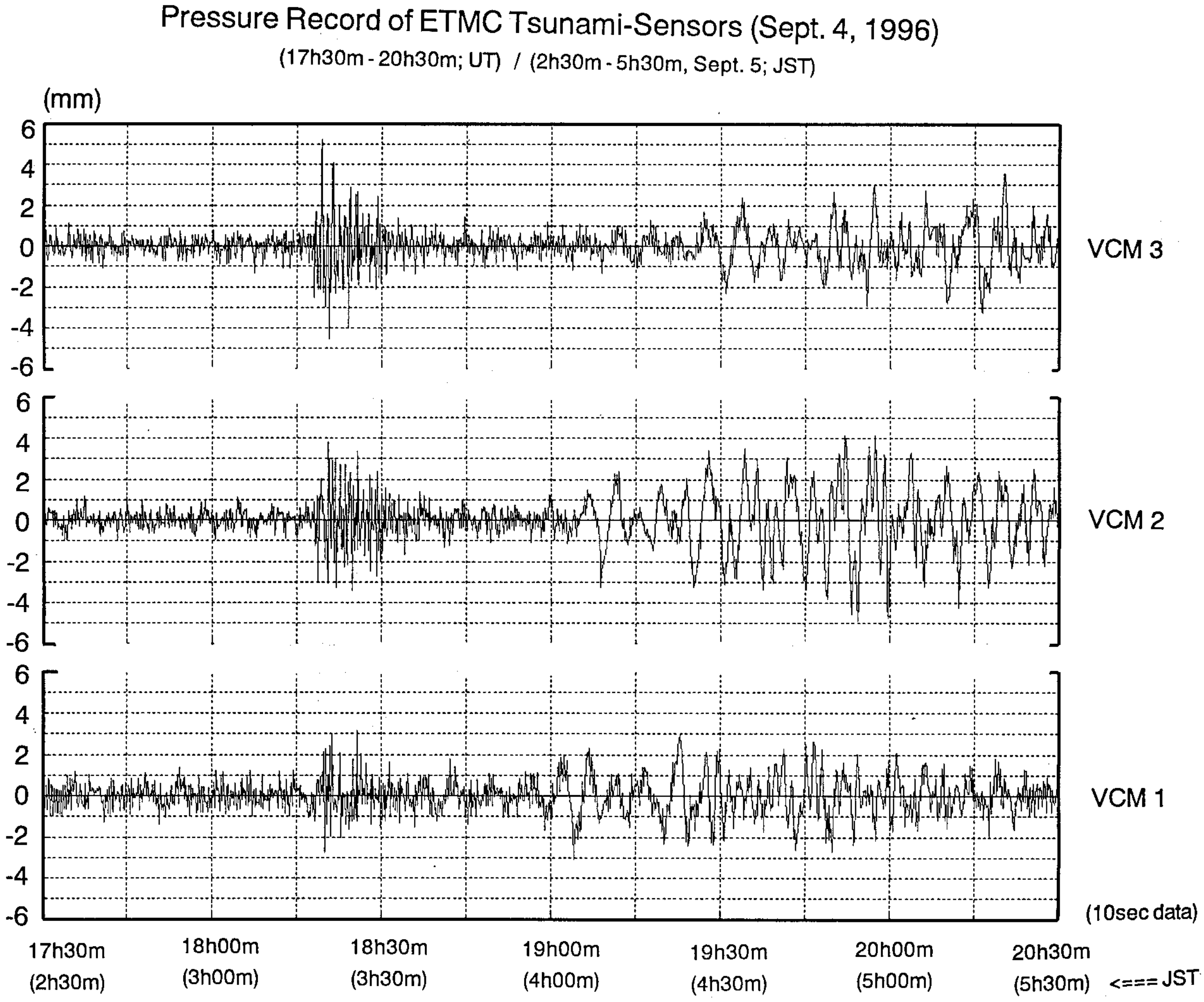

Figure 10. Actual tsunami data obtained from the pressure sensors along the ETMC. The tsunami wave trains originated from a shallow seismic event at 31.4–31.5 N, 139.7–140.0 E with 7.5 Mt (5.7 M_W and 6.2 M_{JMA}) at 18^h16^m on September 4 (UT), 1996. The pressure data are expressed as changes in sea water depth. The original pressure data were sampled at 10 Hz. We transformed the original time series data to a new data set with 10 s sampling intervals, to improve 'data resolution'. Then, we applied a band pass filter to remove 'noises' such as tides. After the approximate time of 19h00m at VCM1 (19^h05^m at VCM2, and 19^h10^m at VCM3), the transformed data show tsunami wave trains with several mm to 1 cm amplitude (P-P) at mm order resolution. Signals with high frequency component from 18^h18^m are due to seismic waves from the event. The epicentral distance between the tsunami event source and the ETMC is approximately 360 km (VCM1) to 420 km (VCM3). The data plotted are for the three hour period from 17^h30^m to 20^h30^m on September 4 (UT), 1996. The local time standard in Japan (JST) is 9 h earlier than UT.

mum amplitude and also before the time of 'trigger off' for the seismic event. The S-P time is larger than 1 s, because the observation sites are underlain by a sedimentary layer thicker than approximately 1 km. It seems that the sedimentary layer has a small ratio of Vs Vp^{-1}. Again, S-P time is less than 40 s. In the event that the S-P time is estimated to be less than 1 s, the system neglects the S-arrival value. The S-time slightly precedes the maximum amplitude arrival time (hereafter, 'Max-time'). This is because the wave section with the maximum amplitude seems to consist of converted S-waves, inhomogeneous S-waves and/or surface waves, etc. Our experience with the ETMC data is that the interval between the S-wave arrival and Max-time is smaller than S-P time on the same channel data for local earthquakes. We are currently setting the ratio, STA LTA^{-1}, at the arrival of S-waves to, for example, 3.5. The value of STA LTA^{-1} influences the degree to which seismic event signals are picked up on the record with noises. Generally, the case of

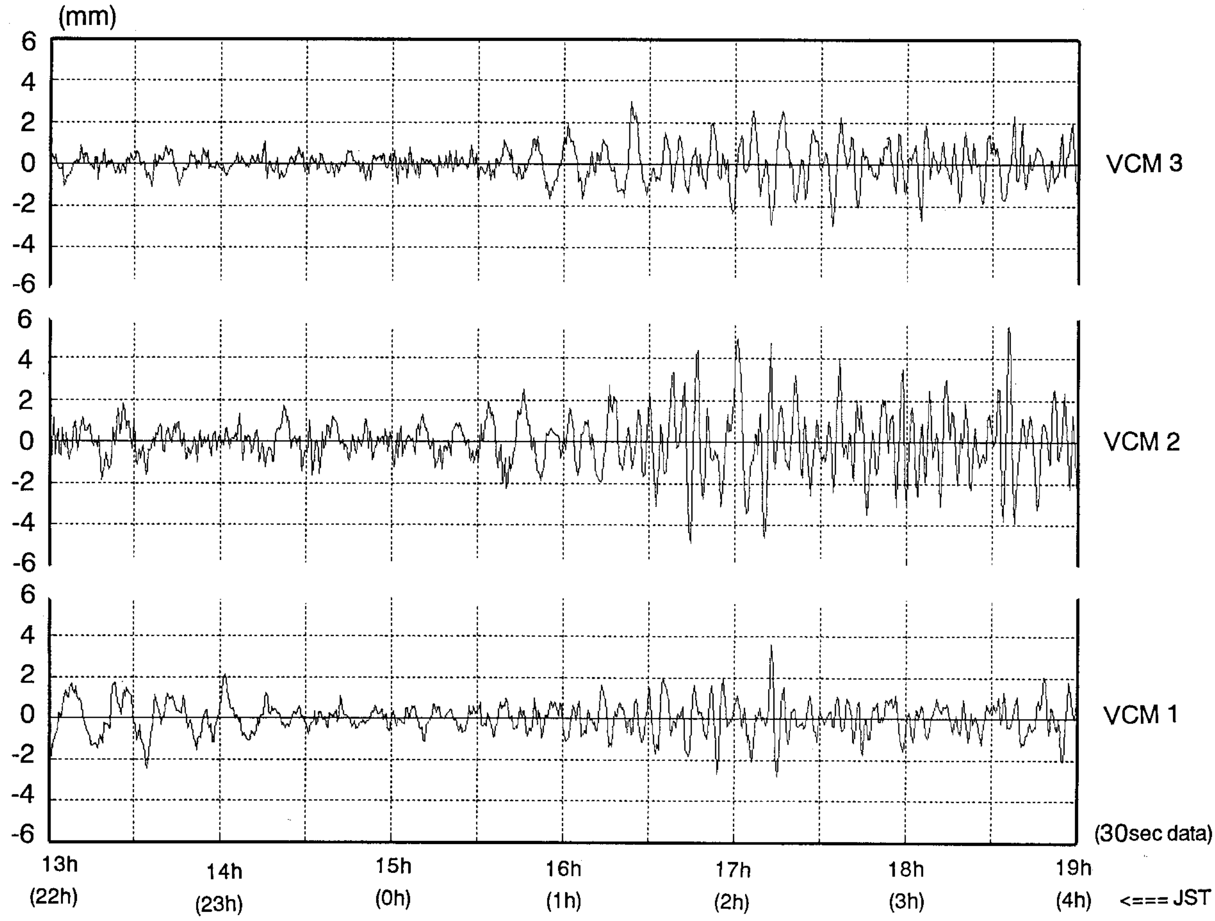

Figure 11. Recent pressure data of the '1998 New Guinea tsunami earthquake' observed with the ETMC. According to the preliminary report of the Centroid-Moment-Tensors by Harvard University (HVD-CMT), the tsunami signals were from the earthquake with 7.1 M_W and 5.2×10^{26} Mo [dyne-cm], at 08^h49^m, July 17, 1998 (UT). The epicenter was approximately at 3 S and 142 E, that is, near the coast of the northern New Guinea, where the Caroline plate (or the North Bismarck sea plate) is subducting to the south. The epicentral distance between the tsunami event source and the ETMC is approximately 4.2×10^3 km. The pressure data shown were processed as in Figure 10, but the original signals are transformed into time series of 30 s intervals. Between 15^h30^m and 16^h00^m, we can recognize the arrivals of tsunamis at VCM2, and VCM3. However, the arrival is not clear on VCM1. Long period noises around 13^h to 14^h30^m on VCM1 was not actual but artificial, that is, due to band-pass filtering process of the abrupt change in pressure at around 13^h 30^m. The maximum tsunami amplitude was approximately 5 mm (0–P). The data plotted are for the six hour period from 13^h00^m to 19^h00^m, July 17, 1998.

larger STA LTA^{-1} is not appropriate to pick up the smaller-magnitude seismic event. Statistical analysis is conducted for all horizontal records of not only velocity seismometers but also accelerometers. In total, for a single station, there are four time series to find the S-wave arrival. For the S-wave arrival, we adopt an estimation with the earliest one among the statistically assigned time points on the four time series. The system has two steps for finding the S-wave arrival on each horizontal channel. At the first step, LTA is measured for the preceding 30 sec, and STA for the preceding 1 s. Then, using AR logic, the system searches for the first-order location of the S-wave arrival around the location of the S-wave with the STA LTA^{-1} value of 3.5. At the second step, the LTA is for the preceding 5 s and STA for 0.1 s. Thus, the S-wave arrival with a scale of 0.1 s for automatic hypocenter calculation can be ascertained. Using the P- and S-wave arrival times etc. the system automatically locates the hypocenters. Here, it must be noted that, during the automatic hypocenter locating process, we utilize only the triggered station data. This is one of the limitations of automatic hypocenter determination.

Next, by carefully reading the P- and S-wave arrivals, we manually re-locate the hypocenters which were located automatically. In this step, we manually read the arrival times on the seismic data not only from triggered stations but also from other non-triggered sites among the submarine sites and land stations, in order to improve the accuracy of the hypocentral parameters. The event magnitude is estimated from the maximum amplitude data of the U/D component of the velocity seismometer.

Next, we compare two maps of automatically located events shown in Figures 9a and 9b, for the same period of nine months from April 1 through December 31, 1997. Figure 9a depicts events which are located with the seismic data of both the six ETMC sites and the nearby thirty selected land stations of NIED. In Figure 1b, the filled circles, 30 in total, shows the selected land stations where the long-term averaged noise levels are not high. Whereas, Figure 9b represents the hypocenters which are determined using mainly the seismic data of NIED land stations in the Kanto-Tokai region. All of the land stations used for the events in Figure 9b are shown in Figure 1b. The total events plotted on Figures 9a and 9b are 2274 and 1267, respectively. Here, it must be noted that the events in Figure 9b are approximately confined north of 33.7 N and west of 141.7 E. This suggests that, for the hypocenter determination, the contribution of oceanic island stations is somehow limited as compared with that of the land sites where the noise levels are relatively low. As is already stated, observation sites on the Izu-Bonin islands show relatively high noise level. The hypocenter determination software, which used to locate events in Figure 9b, usually omits offshore events at areas south of 33.7 N and east of 141.7 E in the Izu-Bonin region. In other words, the software for locating events shown in Figure 9b sets the event-trigger levels of coastal stations to be higher than those in the case of our analyzing system. Regarding at least an offshore region north of 33.7 N and west of 141.7 E, Figure 9a indicates events being approximately two times as many as in Figure 9b. Thus, our system, using both the ETMC and nearby land stations, can reveal the activity of smaller earthquakes in the offshore region around the Izu-Bonin islands.

Here we consider such a case of limited station data available that there are only seismic data from the six ETMC sites, during the hypocenter determination. In this case, the system software would locate only local events, around the linear seismic array of the ETMC, having both the high quality P- ad S-waves' arrival time data. This is partly because the system software assumes a simple, horizontally layered seismic velocity structure, which is similar to that in the Jeffreys-Bullen (1958) table during the hypocenter locating process for earthquakes at the three dimensional, inhomogeneous subduction zone in actual.

We would like to express that the automatically located hypocenters, shown in Figures 9a and 9b, are not final results for detailed studies of local seismicity and their tectonic implications etc. After the process of off-line, manual picking up the P- and S-waves arrivals, we get more precise data set of hypocenters.

Tsunami propagation in the Sagami trough area

As shown in Figure 10, we observed actual tsunami wave trains originating from a recent shallow seismic event at 31.4–31.5 N, 139.7–140.0 E, that is, near Tori-Shima (Tori Is., in other words, Bird Is.) with 5.7 M_W (5.4 M_b, 6.2 M_{JMA}) at 18^h16^m on September 4, 1996. The hypocenter is approximately 360 km away from VCM1 of the ETMC. According to the data compilation by JMA, the tsunami amplitude (P-P), observed at several coastal tide stations around the Sagami trough region, ranged from 5 cm at the south coast site (just north of ST2 of the ETMC) of Boso peninsula, to 16–26 cm at the Izu-Bonin Island arc. For example, the approximate maximum amplitudes (P-P) of the observed tsunamis are 26 cm at Hachijo Is. at18^h58^m, 16 cm at Miyake Is. at 19^h13^m and 20 cm at Oshima Is. at 19^h42^m. Hachijo Is., Miyake and Oshima Is. are all part of the northern Izu-Bonin Island arc. However, few shallow earthquakes with a magnitude less than 7 accompany observable tsunami signals. In this sense, the 1996 tsunami earthquake is a kind of 'anomalous' seismic event. Tsunami magnitude (Mt) determined using the observed tsunami amplitude, was 7.5 (Abe, 1996, unpublished). A larger Mt value than M_W (or than M_{JMA}) value implies that the event was a 'tsunami earthquake' (Kanamori, 1972).

Due to a topographical difference between the coastal tide observation stations above and those along our on-line network, we can infer that the tsunami amplitude (P-P) caused by the event was approximately 1 cm along the ETMC. Actually, the processed data from the ETMC during the tsunami indicate wave trains with an amplitude (P-P) of several mm to 1 cm. The data shown in Figure 10 supports the fact that the tsunami sensors of the ETMC can provide data with a resolution of approximately 1 mm order. This high resolution of pressure data provides information regarding sea level changes and/or crustal uplift for periods less than a year, although calibration of the secular change in the sensor response must be carried out to elucidate the actual change precisely.

On June 13, 1984, a similar tsunami earthquake occurred near 31.5 N, 139.7–140.0 E with 7.3 Mt (5.6 M_W, 5.9 M_{JMA} and 5.5 m_b). Analysis of the seismic wave form data by Kanamori et al. (1993) suggests that the 1984 tsunami earthquake originated from some volume source change such as 'magma intrusion' toward the shallow sedimentary layer. A simple interpretation is that the tectonic background for both the tsunami earthquakes at Bonin Island arc in 1984 and 1996 might be similar. Both the 1984 and 1996 tsunami events occurred around the back-arc extensional depression zone just west of the volcanic front along the Izu-Bonin arc. During the observation period from April through December 1996, as for the actual tsunami record, we could save only the above information for September 4, partly because of artificial trouble with the tsunami data recording process. We have been continuously recording the water pressure data from the ETMC since early 1997.

Recently, at 08^h49^m, July 17, 1998 (UT), there was a large tsunami event (hereafter, '1998 New Guinea tsunami earthquake') near the northern coast of New Guinea Is, that is approximately at 3 S and 142 E. The large tsunamis associated with the event killed more than 3 thousand people. Figure 11 represents the pressure data of the 1998 New Guinea tsunami earthquake observed with the ETMC. According to the preliminary report of the Centroid-Moment-Tensors by Harvard University (HVD-CMT), the tsunami earthquake was of 7.1 M_W and 5.2×10^{26} Mo [dyne-cm]. The epicenter was at the plate convergence zone between the Indo-Australia and Caroline (or North Bismarck sea) plates. The maximum tsunami amplitude among the VCM1, 2, and 3, was approximately 5 mm (0-P), although the arrivals are relatively less clear than those in Figure 10 partly because of the longer epicentral distance. According to the data of several coastal tide stations around the Sagami trough region, compiled by JMA, it seems that the tsunamis arrived at just before and after 16^h (1^h JST), and their amplitudes (P-P) were 20–30 cm.

Conclusion

After five years preparation in early 1996, we deployed an on-line operating cable network of seismometers and tsunami sensors at the Sagami trough subduction zone, south of the Tokyo metropolitan area. The network, called ETMC, provides on-line seismic data with a wide dynamic range, because two types of seismometers are mounted at each seismic observation point. So far, the ETMC is one of the most up-to-date and sophisticated on-line marine seismic network. The average observed noise level is smaller than for other previously existing marine seismic networks around the Japanese island arc. Although, the present stage is considered to be within the quiescent stage during the great earthquake cycle at the Sagami trough subduction zone, the analysis of data from the ETMC and nearby land seismic stations reveals the actual site and activity of microearthquakes within the Philippine sea plate and the overriding plate. The tsunami sensors recorded water pressure changes due to 'tsunami earthquakes' at a resolution of mm order.

The ETMC plays an important role in the monitoring of seismicity and the tsunami propagation process at the Sagami trough subduction zone and its vicinity.

Acknowledgements

The ETMC project at NIED was conducted with the continuous support and encouragement of the STA (Science and Technology Agency), Japan and fishery organizations as well as of local governments in Hiratsuka city, Kanagawa prefecture and Tokyo etc. NEC corporation assisted us not only during the manufacture of the most part of the ETMC but also during the process when the system was laid on the seafloor. NTT corporation assisted us during the cable deployment using their cable operation ship, *Kuroshio-Maru*.

References

Eguchi, T., Fujinawa Y., Matsuzaki T. and Aoyagi M.: 1986, 'New Pop-up Type Ocean Bottom Seismometer', *Mar. Geophys. Res.* **8**, 187–199.

Eguchi, T., Fujinawa Y. and Ukawa M.: 1987, 'Microearthquakes and Tectonics Around an Outer Rise: the Zenisu Ridge, Japan', *Phys. Earth Planet. Inter.* **48**, 47–63.

Eguchi, T. and Fujinawa Y.: 1991, 'New projects with on-line sea-bottom cable observation system for monitoring crustal activity in off-shore areas by the National Research Institute Earth Science and Disaster Prevention', *The Kaiyo Monthly* **23**, 321–328 (in Japanese).

Jeffreys, S. H. and Bullen, K. E.: *Seismological Tables*, British Assn. Advans., Gray-Milne Trust.

Kanamori H.: 1971, 'Faulting of the great kanto earthquake of 1923 as revealed by seismological data', *Bull. Earthquake Res. Inst.* **49**, 13–18.

Kanamori H.: 1972, 'Mechanisms of Tsunami earthquakes', *Phys. Earth Planet. Inter.* **6**, 346–359.

Kanamori, H., Ekstrom G., Dziewonski A., Barker J. S. and Sipkin S. A.: 1993, 'Seismic radiation by magma injection: an anomalous seismic event near Tori Shima, Japan', *J. Geophys. Res.* **98**, B4, 6511–6522.

Matsu'ura, M, Iwasaki T., Suzuki Y. and Sato R.: 1980, 'Statical and dynamical study on faulting mechanism of the 1923 Kanto earthquake', *J. Phys. Earth* **28**, 119–143.

Seismology and volcanology research division, Meteorological research institute (MRI), Japan: 1980, 'Permanent ocean-bottom seismograph observation system', *Technical Reports of the Meteorological Research Institute*, No. **4**, p. 233 (in Japanese).

Ukawa, M., Eguchi T. and Fujinawa Y.: 1989, 'Seismicity survey with pop-up type OBS array in the western part of Sagami Bay', *J. Phys. Earth* **37**, 31–54.